Rapidity Dependence of Chemical Freeze–out in Au–Au Collisions

Kristen Parzuchowski
Research Experience for Undergraduates
Wayne State University

August 7, 2015

Abstract

The study of nuclear matter is possible using heavy ion collisions. The part of the collision that is measurable is just after chemical freeze–out, where the interaction between produced particles cease. There are several methods that locate where this freeze–out occurs, however they do not account for rapidity. This study focuses on the rapidity dependence of baryon chemical potential and temperature extracted using cumulants of central UrQMD simulated events to compare to Lattice Quantum Chromodynamics. There was a significant rapidity dependence found.

1 Introduction

The quantum chromodynamic (QCD) phase diagram depicts hadronic and quark gluon plasma matter depending on density (baryon chemical potential μ_B) and temperature (T) (see Figure 1). The diagram is still speculative because the critical point and first order phase transition have yet to be observed. The study of heavy ion collisions is necessary to learn more about nuclear matter. In these collisions increasing the beam energy lowers μ_B. The yellow paths on the phase diagram are the paths taken by a system after a collision. After quark gluon plasma is formed hadronization occurs and then chemical freeze–out. Chemical freeze–out is when the inelastic collisions between the particles stop. The multiplicities of the hadrons stay constant at this point. After chemical freeze–out, kinetic freeze–out occurs, which is when the hadrons stop interacting and the momenta of the particles stays constant.

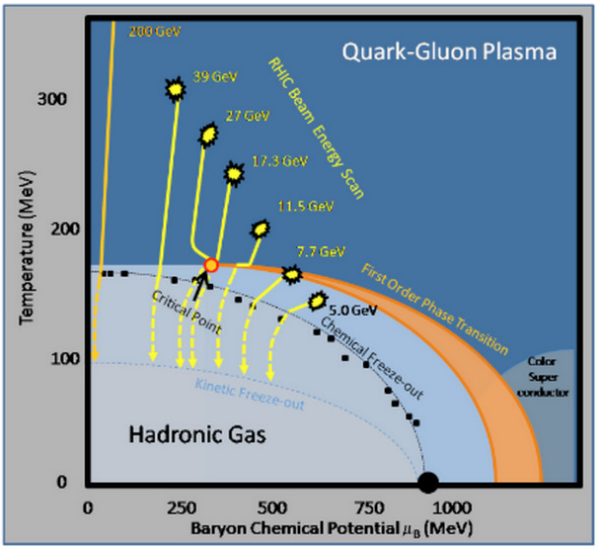

Figure 1: The QCD phase diagram

One can infer where chemical freeze–out occurs on the phase diagram using several methods: Statistical Hadronization Models (SHM) ([1],[2],[3]), Hadron Resonance Gas models (HRG) ([4],[5]), and cumulants compared to Lattice QCD (LQCD) ([6]). These approaches have previously ignored the rapidity dependence, and/or averaged over different experiments with different rapidity acceptances.

This study analyzes the rapidity dependence of the (μ_B,T) values extracted using cumulants compared to LQCD in UrQMD simulated events and compared the results to the other approaches. The rapidity of a particle is defined as,

$$y = \frac{1}{2} ln \left(\frac{E + p_z}{E - p_z} \right)$$

and the psuedorapidity is defined as,

$$\eta = -ln \left[tan \left(\frac{\theta}{2} \right) \right]$$

where y is the rapidity, E is the energy, p_z is the momentum along the beam axis, η is the psuedorapidity ($\approx$ rapidity at relativistic speeds) and θ is the angle between the particle three-momentum and the positive direction of the beam axis.

In this study, Ultra-relativistic Quantum Molecular Dynamics (UrQMD) was used to generate realistic events. The events were central collisions at beam energies, $\sqrt{s_{NN}}$, of 7.7, 11.5, 14.5, 19.6, 27, 39, 62.4 and 200 GeV. These beam energies are the same as the real data collected by the STAR experiment at Brookhaven National Labratory.

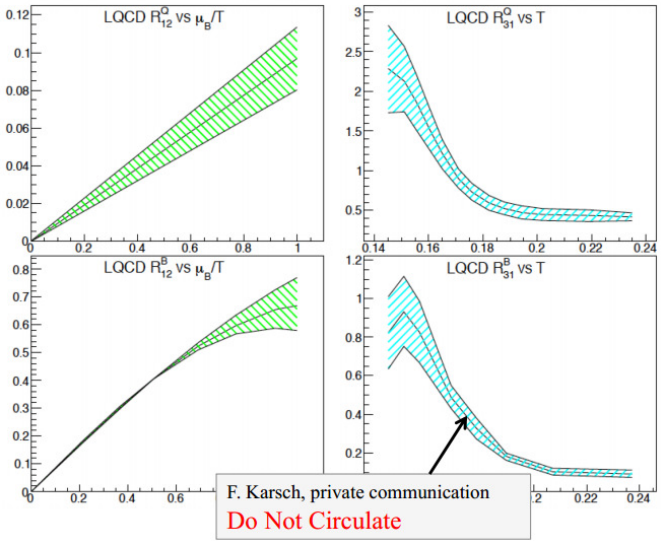

Figure 2: LQCD predictions

2 Methods

Lattice QCD calculates conserved quantities like baryon number (B) and total charge (Q). We calculated the cumulants (C_1, C_2, C_3) and ratios of cumulants (R_{12}, R_{31}) of the multiplicity distributions of net baryon number and net charge, e.g. $N_B - N_{\overline{B}}$. We use "net" quantities to avoid contribution from associated production, where proton-antiproton pairs are produced. The observables of interest are defined as,

$$C_1 = M, \qquad C_2 = \sigma^2, \qquad C_3 = S,$$
$$R_{12} = \frac{C_1}{C_2}, \qquad R_{31} = \frac{C_3}{C_1},$$

where R_{12} is the ratio $\frac{C_1}{C_2}$ (mean divided by the variance), M is the mean, σ is the variance, S is the skewness and C_i are the cumulants.

We were then able to compare these ratios to LQCD predictions and infer μ_B/T from the given data set. In Figure 2, the LQCD predictions are shown comparing either R_{12} with μ_B/T values or R_{31} with T values. The two upper plots correspond to net-Q cumulant ratios whereas the two lower plots correspond to net-B cumulant ratios. The average inferred LQCD value is taken for a given experimental cumulant ratio. These inferred values were plotted in different ways that allowed us to look at the values based on rapidity acceptances and look for trends. We then compared the results to other approaches.

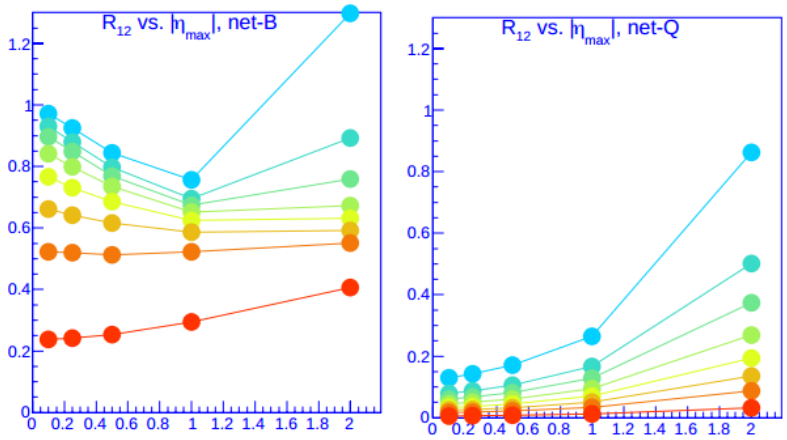

(a) Net-B (b) Net-Q

Figure 3: R_{12} vs. $|\eta_{max}|$

3 Results

In Figure 3, the cumulant ratio R_{12} from net-B and net-Q is compared to $|\eta_{max}|$. Each colored line corresponds to a different beam energy, which is shown in Figure 4. R_{12} is increasing as $\sqrt{s_{NN}}$ increases. The values in these plot were then compared to Lattice QCD predictions.

The μ_B/T values were extracted from LQCD and plotted in Figure 5 against $|\eta_{max}|$ with the colors corresponding to the same beam energies shown in Figure 4. Figure 5-a shows μ_B/T increasing with increasing rapidity acceptances for higher beam energies whereas 5-b shows μ_B/T increasing with increasing rapidity acceptances for all beam energies. This is a significant rapidity dependence.

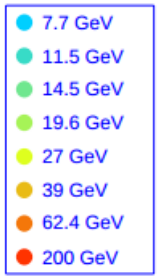

Figure 4: Key for Figures 3 and 5

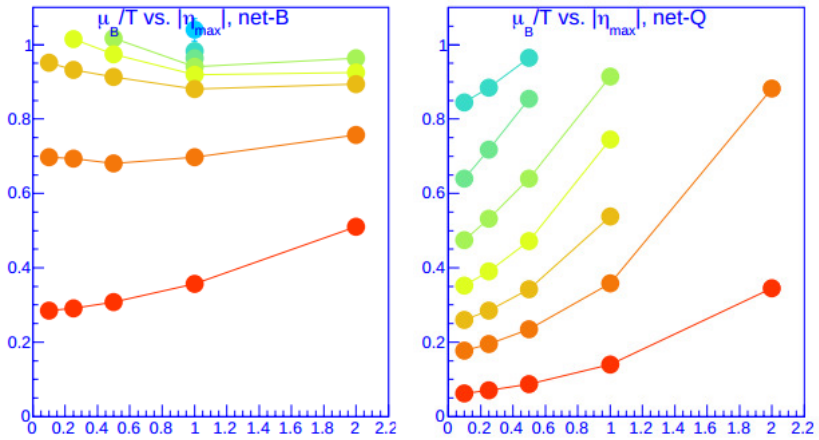

(a) Net-B (b) Net-Q

Figure 5: μ_B/T vs. $|\eta_{max}|$

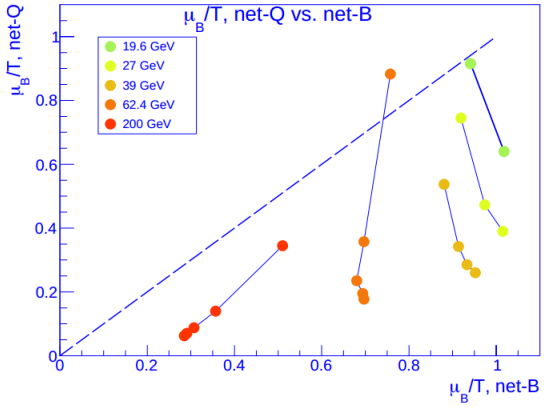

Figure 6: μ_B/T from Net-Q vs. μ_B/T from Net-B

In Figure 6, μ_B/T from net-Q is compared to μ_B/T from net-B. The dotted diagonal line is a line of reference with a slope of 1. Each data point represents a μ_B/T value from net-B and net-Q at the same beam energy and the same rapidity acceptance. The data is generally in the lower triangle, hence net-B values are generally higher. These values are expected to be plotted along the diagonal, but μ_B/T from net-B is notably different when compared to μ_B/T from net-Q at the same beam energy and rapidity acceptance. This plot shows significant rapidity dependence because each μ_B/T data point from a certain rapidity acceptance shows a vastly different value than all of the other μ_B/T

data points of the same beam energy with different rapidity acceptances.

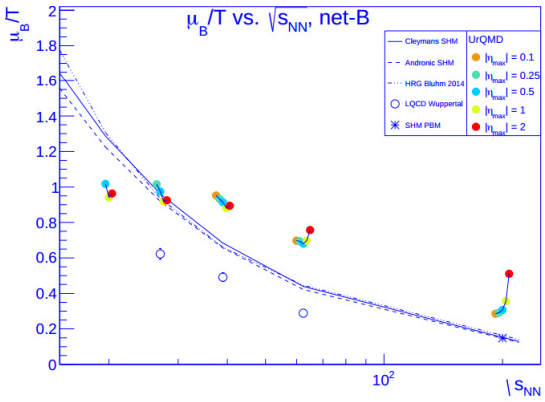

(a) Net-B

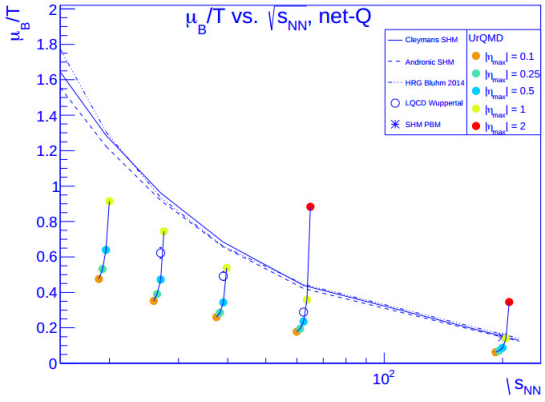

(b) Net-Q

Figure 7: μ_B/T vs. $\sqrt{s_{NN}}$ compared with other approaches

Figure 7 shows μ_B/T from net-B and net-Q compared to $\sqrt{s_{NN}}$ on a log scale. These plots also takes other approaches into account. The blue downward sloped lines in this figure are from SHM and HRG approaches, and the open–circled data points are from an LQCD approach using experimental data. The colorful points are the UrQMD data points plotted at different rapidity acceptances. Data from all of the approaches follows a general downward slope that agrees with the assumption that μ_B/T decreases with increasing beam energy. All of these approaches give notably different values for μ_B/T. The UrQMD μ_B/T from net-B is generally above the parameterizations from other approaches whereas μ_B/T from net-Q is generally below. The UrQMD data points for different rapidity acceptances demonstrate how unique the μ_B/T values are at each acceptance and thus provide another figure that shows significant rapidity dependence.

4 Discussion

The results of this study confirm that there is a significant rapidity dependence in chemical freeze–out parameters extracted from simulated data. The values of μ_B/T from net-B were found to be less sensitive to the rapidity acceptance than those from net-Q. They were also generally larger than net-Q μ_B/T values. It was observed that all of the studied approaches gave differing results. Rapidity is typically ignored, however it can be a deciding factor in the experimental events' locations on the QCD phase diagram. Continuing work can be done on this project through analyzing the rapidity dependence using other models aside from UrQMD. Eventually this technique should be applied to actual data from the STAR detector.

5 Acknowlegdements

This work was performed as part of the 2015 Wayne State University Research Experience for Undergraduates (REU) program funded by the US National Science Foundation. This program was led by Professors A. Petrov and D. Cinabro. Helpful comments on the present analysis were provided by Professor W.J. Llope and fellow REU participant Isaac Pawling.

References

[1] A. Andronic *et al.* (2012), arXix:1210.7724 [nucl-th].

[2] A. Andronic. "Hadron production at chemical freeze–out and the QCD phase diagram". July 2010. PowerPoint presentation.

[3] J. Cleymans *et al.* (2005), arXiv: hep-ph/0511094.

[4] M. Bluhm *et al.* (2014), arXiv:1412.5934 [hep-ph].

[5] P. Alba *et al.* (2014), arXiv:1403.4903 [hep-ph].

[6] S. Borsányi *et al.* (Wuppertal-Budapest). Phys. Rev. Lett. 111, 062005 (2013).